ChemComm

Accepted Manuscript

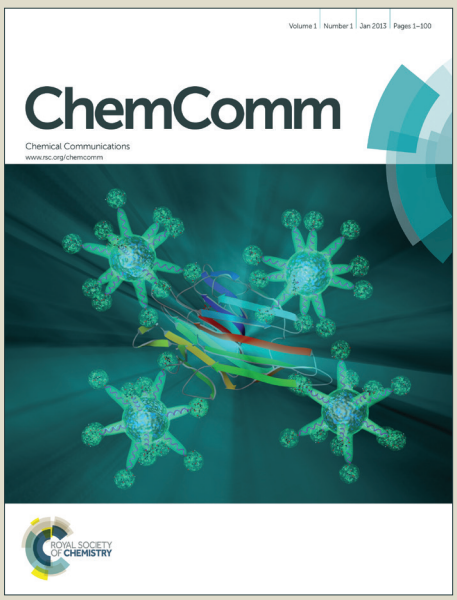

ROYAL SOCIETY OF CHEMISTRY

www.rsc.org/chemcomm

Cite this: DOI: 10.1039/c0xx00000x

www.rsc.org/xxxxxx

ARTICLE TYPE

Two Carboxyethyltin Functionalized Polyoxometalates for Assembly on Carbon Nanotubes as Efficient Counter Electrode Materials in Dye-Sensitized Solar Cells †

Xiao-Jing Sang,‡[b] Jian-Sheng Li,‡[b] Lan-Cui Zhang,*[a] Zai-Ming Zhu,[a] Wei-Lin Chen,*[b] Yang-Guang Li,[b] Zhong-Min Su,[b] En-Bo Wang*[b]

Received (in XXX, XXX) Xth XXXXXXXXX 200X, Accepted Xth XXXXXXXXX 200X

DOI: 10.1039/b000000x

Two novel open-chain carboxyethyltin decorated sandwich-type germanotungstates have been successfully synthesized. They could markedly increase the electrocatalytic activity of single-walled carbon nanotube toward triiodide reduction when assembled into composite electrodes, which have shown a conversion efficiency of 6.32% that is comparable to that of Pt electrode (6.29%) when used as counter electrodes in dye-sensitized solar cells.

Dye-sensitized solar cells (DSSCs) are among the most promising photovoltaic devices capable of addressing the future energy crisis owing to simple fabrication procedures, environmental friendliness and relatively high efficiency.[1] As a crucial component in DSSCs, the counter electrode (CE) performs two functions consisting of promoting the electron translocation from the external circuit and catalyzing the reduction of I_3^- to I^-.[2] Although Pt is the effective CE material for DSSCs, the restrictions of noble metal creates a big obstacle for scale-up application of DSSC devices. Therefore, it is urgent to develop Pt-free CE materials with both low cost and relatively high efficiency. Poly(3,4-ethylenedioxythiophene) (PEDOT) has shown promise with Co(III/II) mediators and organic mediators especially as an alternative Pt free CE material.[3]

Carbon nanotubes (CNTs), consisting of single-walled nanotubes (SWNTs), double-walled nanotubes (DWNTs) and multi-walled nanotubes (MWNTs), have become potential candidates for use as alternative counter electrode materials in DSSCs owing to their excellent combination of properties such as high electrical conductivity, large surface area and abundance.[4] Nevertheless, to optimize their catalytic activity aiming to further improve the conversion efficiency still remains one challenge.[5]

Polyoxometalates (POMs) are a class of molecular-scale transition metal-oxygen nanoclusters based on abundant elements,[6] which have attracted extensive interest in the fields of magnetism, optics and materials chemistry because of their unique structural topologies and versatility such as magnetic properties,[7] nonlinear optics,[8] catalytic activity,[9] electrochemical properties.[10] Organotin decorated POMs are a unique class of organic-inorganic functionalized POM-based derivatives which possess excellent electrocatalytic activities and and semiconductor like features.[11] Organotin decorating would induce the variation of charge density of oxygen ions on the surface of POMs, which could adjust the electronic characteristic and redox catalytic properties of POMs. In addition, the organic functional groups provide a new opportunity for the further loading of POMs. Thereby, POM-organotin derivatives are promising modifiers for CEs of DSSCs. Applying them to modify CNTs are expected to obtain high-performance CEs with both high conductivity and catalytic activity. Nevertheless, no attention has been dedicated to this application of organotin modified POMs to date.

Herein, two novel open-chain carboxyethyltin functionalized germanotungstates $\{C(NH_2)_3\}_{10}H_2[Cu_2\{Sn(C_3H_4O_2)\}_2(B\text{-}\alpha\text{-}GeW_9O_{34})_2]\cdot 7H_2O$ (**GeW_9-Cu-SnR**) and $\{C(NH_2)_3\}_{10}H_2[Co_2\{Sn(C_3H_4O_2)\}_2(B\text{-}\alpha\text{-}GeW_9O_{34})_2]\cdot 8H_2O$ (**GeW_9-Co-SnR**) were designed and synthesized in aqueous solution and characterized by physical and chemical methods (Fig. 1, Fig. S1-S12, Table S1-S5, see ESI†). They were applied for modifying SWNT to fabricate SWNT/POM composite electrodes via electrodeposition, which show higher electrocatalytic activities toward reduction of I_3^- and higher conversion efficiency when used as CEs in DSSCs than SWNT-only electrodes. It is important that the performances of DSSCs with SWNT/ **GeW_9-Cu-SnR** and SWNT/ **GeW_9-Co-SnR** CEs are superior to ones with SWNT/ GeW_9 and SWNT/ GeW_9Cu_4 CEs, although their efficiencies are all higher than pure SWNT-based cells. This indicated that organotin groups could exert a positive impact on the electrocatalytic activities of POMs. Notably, SWNT/ **GeW_9-Co-SnR** and SWNT/ **GeW_9-Cu-SnR** have shown the high conversion efficiency of 6.20% and 6.32% as the CEs respectively, which are comparable to that of Pt CE (6.29%).

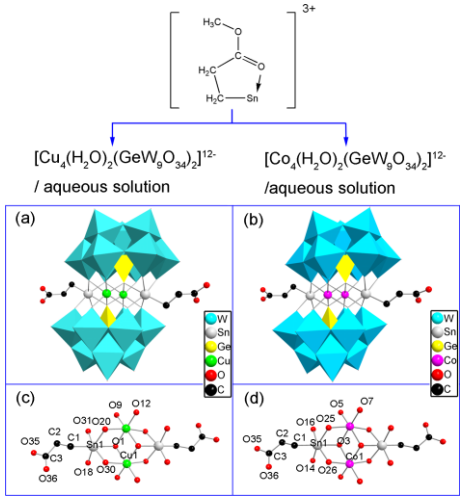

Fig. 1 Schematic representation of the preparation of (a) **GeW_9-Cu-SnR**; (b) **GeW_9-Co-SnR**.

Single-crystal X-ray diffraction analysis reveals that both the polyoxoanions of **GeW_9-Cu-SnR** and **GeW_9-Co-SnR** display the sandwich-type structure and they are isostructural. Thereby **GeW_9-Cu-SnR** is described as an example below. In **GeW_9-Cu-SnR** (Fig. 1a), two B-α-$[GeW_9O_{34}]^{10-}$ are combined with two $[Sn(CH_2)_2COO]^{2+}$ moieties and two Cu^{2+} cations by sharing corner O atoms of WO_6 octahedra and GeO_4 tetrahedra. Two Cu^{2+} cations and two $[Sn(CH_2)_2COO]^{2+}$ moieties are located in the inner and outer positions in central core of the compound, respectively. Each $[Sn(CH_2)_2COO]^{2+}$ unit links two B-α-$[GeW_9O_{34}]^{10-}$ units *via* five terminal oxygen atoms from two POM units, forming hexa-coordinated environments for two Sn centers (Sn1 and its symmetrical equivalent position). The Sn–C distance is 2.153(14) Å, and the Sn–O distances are in the range of 2.042(6)-2.340(6) Å. Each Cu^{2+} ion is six-coordinated by six terminal oxygen atoms derived from two B-α-$[GeW_9O_{34}]^{10-}$ units. The Cu–O distances are in the range of 1.941(7)-2.334(7) Å. Besides, the estertin precursor $[Sn(CH_2)_2COOCH_3]^{3+}$ hydrolyses into open-chain carboxyethyltin $[Sn(CH_2)_2COO]^{2+}$ during the reaction process, such a phenomenon has ever been observed in our recent report. The exposed carboxyl-terminal group could provide new opportunity for the POM-carboxyethyltin derivatives further functionalized by linking with metal cation or organic group. For the packing arrangement of **GeW_9-Cu-SnR**, the adjacent sandwich-type polyoxoanions are stacked into a 3-D supramolecular framework *via* the extensive H-bonding interactions.

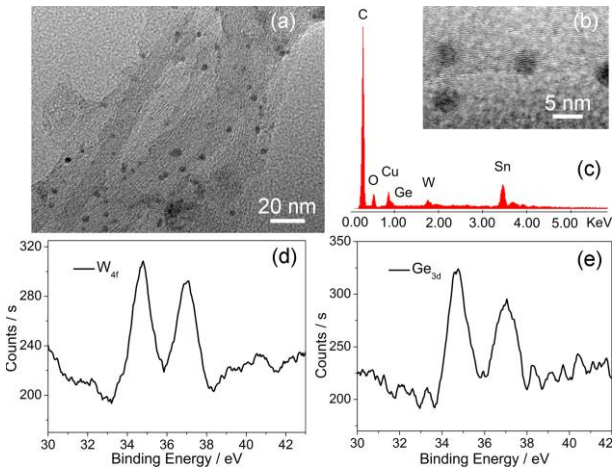

Fig. 2 (a) HRTEM and (b) High magnification HRTEM image of SWNT/ **GeW_9-Cu-SnR**; (c) EDS and (e), (f) XPS spectrum for SWNT/ **GeW_9-Cu-SnR**.

Electrodeposition method was employed to assemble POMs on the SWNT electrode which was prepared by screen printing in advance. Briefly, SWNT paste was obtained by grounding SWNT powder in a mixture of glacial acetic acid, ethanol, terpineol and ethylcellulose and was then deposited on the cleaned FTO glass by screen printing, followed by heating at 300 °C for 15 min.[12] The hybrid electrode was fabricated by cyclic potential scanning from 0.2 V to -1.2 V, followed by washing with deionized water thoroughly and drying in a N_2 stream. The obtained hybrid films were characterized by HRTEM, EDS, XPS, Raman (Fig. S14-19, ESI†). A 12μm thick TiO_2 film (P25, Degussa, Germany, Fig. S20) sensitized by N719 was used as the photoanode (details see ESI†).

In the Raman spectrum for SWNT (Fig. S13, ESI†), its dominant D band (1410 cm^{-1}) and G band (1596 cm^{-1}) could be clearly observed.[13] For **GeW_9-Cu-SnR**, the band around 1098 cm^{-1} was associated with the stretching mode of W-O_t.[14] For SWNT/ **GeW_9-Cu-SnR**, the G band for SWNT becomes weaker, which is in good agreement with the results reported elsewhere. Notably, the new peaks at 620 and 1100 cm^{-1} for the hybrid film could demonstrate the successful incorporation of polyoxoanions on the SWNT electrode. HRTEM images of SWNT/ **GeW_9-Cu-SnR** were collected to investigate their structure in detail. Fig. 2a illustrates the presence of wispy carbon nanotubes, on the surface of which many nanoparticles are dispersedly loaded with the size of around 3.5 nm (Fig. 2b), which are presumed to be the aggregations of POM anions. Fig. 2c shows the element distribution of SWNT/ **GeW_9-Cu-SnR** which was detected by EDS analysis. Obviously, the peaks for tungsten, germanium, tin and copper could confirm the immobilization of **GeW_9-Cu-SnR** on SWNT. Further, the hybrid contains 7.33 wt% of tungsten as detected by EDS. XPS was also used to determine the existence of POMs and their oxidation states in the hybrid film. From Figs. 2d and 2e, the binding energies of W_{4f} of **GeW_9-Cu-SnR** are located at 34.7 eV and 37.1 eV, respectively, which are consistent with the W^{VI} oxidation state.[15] The two peaks at *ca.* 34.7 eV and 37.0 eV are assigned to the XPS spectrum for Ge_{3d}.[16] The above results suggested that **GeW_9-Cu-SnR** could be immobilized on SWNT *via* electrodeposition and they exist on the surface of SWNT in the form of oxidation state.

The electrocatalytic performances toward triiodide reduction of different electrodes including SWNT, SWNT/ GeW_9, SWNT/ GeW_9-Cu_4, SWNT/ **GeW_9-Co-SnR** and SWNT/ **GeW_9-Cu-SnR** were evaluated through cyclic voltammetry (CV), electrochemical impedance spectroscopy (EIS) and Tafel polarization. Identical conditions were used for Pt electrode as reference.

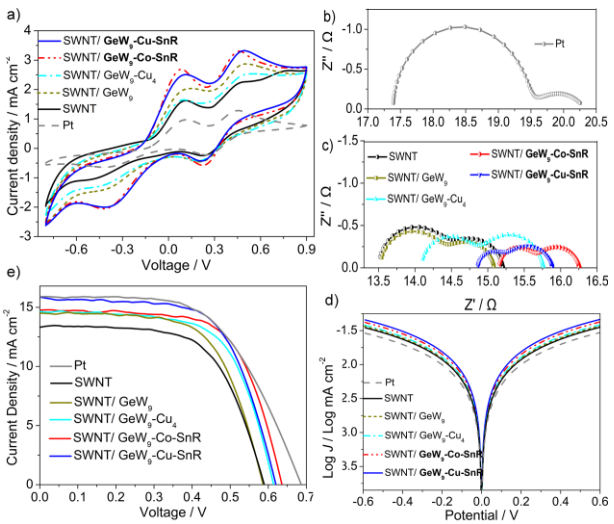

Fig. 3 (a) Cyclic voltammograms for the I^-/I_3^- redox reaction of different CEs; (b) Nyquist plot of Pt CE; (c) Nyquist plots of differen SWNT-based CEs; (d) Tafel polarization curves; (e) *J-V* curves of DSSCs using different CEs.

There are usually two pairs of redox peaks in CV curves, which correspond to oxidation and reduction of I^-/I_3^- and I_3^-/I_2 from left to right.[17] The peak current and the value of peak-to-peak separation between the anodic and cathodic peaks (*E*pp) are two critical parameters for evaluating the catalytic activity of a CE. As shown in Fig. 3a, for SWNT CE, the cathodic peak that was associated with the triiodide reduction was not obvious, indicating the reaction was slow, although it's the key step occurring on the CEs in DSSCs. However, the peak current

increased and the *E*pp relating to redox of I^-/I_3^- decreased significantly after modifying SWNT by POMs, and especially for **GeW_9-Cu-SnR** and **GeW_9-Co-SnR** which even exhibit smaller *E*pp than Pt CE. Besides, modifying SWNT with the organotin fragment $Cl_3SnCH_2CH_2COOCH_3$ (SnR) could also reduce the *E*pp and improve the cathodic peak current involving reduction of I_3^- (Fig. S21-22, Table S7, see ESI†). This phenomenon explained that POMs could improve the electrocatalytic activity as the modifiers of SWNT CE, and POM-organotin derivatives exhibit more remarkable effect, which could be attributed to the additional contribution by the organotin fragment as another catalytic site. Figs. 3b and 3c show the Nyquist plots obtained by EIS measurements using symmetrical cells consisting of two identical CEs. The high-frequency intercept on the real axis represents the series resistance (R_s), the left semicircle region mainly relates to the charge transfer resistance (R_{ct}) at the electrode-electrolyte interface, and the right semicircle region is attributed to Nernst diffusion process of triiodide ions.[18] Various impedance parameters could be obtained by fitting the Nyquist plots and listed in Table S6. It can be concluded that the incorporation of POMs could lead to an obvious reduction of R_{ct} which follows the bellow order: SWNT < SWNT/ GeW_9 < SWNT/ GeW_9-Cu_4 < SWNT/ **GeW_9-Co-SnR** < SWNT/ **GeW_9-Cu-SnR**, although they resulted in slight increasement of series resistance R_s. In general, a decrease in the interface resistance R_{ct} resulted in the enhanced electrocatalytic activity of CEs towards reduction of I_3^-, which further confirmed the results obtained from CV curves. Fig. 3d shows the Tafel polarization curves, which plots the logarithmic current density (log *J*) as a function of voltage. Comparing the curves, the curve for SWNT/ **GeW_9-Cu-SnR** exhibits the largest exchange current density J_0 on the electrode surfaces in the Tafel zone. As documented in literature, J_0 varies inversely with R_{ct}.[19] Thereby, the results by J_0 were in good agreement with that of EIS.

Table 1. Photovoltaic parameters for the DSSCs based on various CEs with N719 sensitizer and I_3^-/I^--based mediator.

	V_{oc}, mV	J_{sc}, mA cm^{-2}	*FF*	PCE, %
SWNT	589	13.48	0.626	4.97
SWNT/ GeW_9	587	14.47	0.640	5.44
SWNT/ GeW_9-Cu_4	614	14.73	0.647	5.85
SWNT/ **GeW_9-Co-SnR**	636	14.72	0.662	6.20
SWNT/ **GeW_9-Cu-SnR**	620	15.80	0.646	6.32
Pt	687	15.92	0.575	6.29

Fig. 3e shows the photocurrent–voltage (*J*-*V*) curves of the DSSCs using different CEs with N719 sensitizer and I_3^-/I^--based mediator. The detailed photovoltaic parameters are summarized in Table 1. To assess the reproducibility of the DSSCs with various CEs, five set of parallel experiments were carried out for each kind of CE, and an average data of these results and the standard deviation derived from the average value are summarized (Tables S8-S13). The photovoltaic characteristics for the cells and the corresponding error bar are shown in Fig. S23-S24. The *J*-*V* curves in Fig. 3e represent the set of data mostly close to that with the average efficiency. It can be concluded that the performances of the DSSCs with SWNT/ POMs hybrid CEs were enhanced compared with ones with SWNT-only CE. Notably, when SWNT/ **GeW_9-Cu-SnR** was applied as CE, the conversion efficiency of 6.32% was produced, with short-circuit current density (J_{sc}) of 15.80 mA cm^{-2}, an open-circuit voltage (V_{oc}) of 620 mV and a fill factor (*FF*) of 0.646, which could be comparable to that of Pt CE that renders a J_{sc} of 15.92 mA cm^{-2}, V_{oc} of 687 mV, *FF* of 0.575 and an efficiency of 6.29%. The DSSCs with SWNT/ **GeW_9-Co-SnR** CEs showed a slight lower efficiency (6.20%), whereas the SWNT-only CE gave an efficiency of 4.97%. Meantime, modifying with GeW_9 and GeW_9Cu_4, the precursor of **GeW_9-Cu-SnR**, both exhibited the positive effect relative to the pure SWNT CE, although they produced the lower efficiency than **GeW_9-Cu-SnR**, which was possibly resulted from their lower electrocatalytic activity. Thereby, SWNT/ **GeW_9-Cu-SnR** or **GeW_9-Co-SnR**, fabricated by anchoring POMs on the SWNT electrode via electrodeposition, could be the promising alternatives to the conventional Pt electrode in DSSCs.

In addition, the electrocatalytic performance of these composite electrode was evaluated under another system employing Z907 sensitizer with a Co(III/II) based mediator when used as CEs of DSSCs. Similarly, five set of parallel experiments were carried out for each CE to perform statistical analysis (Figs. S25-S27, Tables S14-S19). The results show that the performance is greatly enhanced by employing the composite electrode SWNT/ **GeW_9-Co-SnR** or SWNT/ **GeW_9-Cu-SnR** as CEs when using Z907 sensitizer with a Co(III/II)-based mediator. Especially, the *FF* of DSSC with SWNT/ **GeW_9-Co-SnR** as the CE was increased by 30.3% with the PCE increased by 38.9% compared with ones using SWNT-only CE although the PCE was still inferior to that of Pt-based cells. These results demonstrated that the two POM-carboxyethyltin derivatives could also improve the catalytic activity of SWNT electrode toward reduction of the Co(III) component. Furthermore, the precursor of **GeW_9-Cu-SnR,** GeW_9-Cu_4 could improve the J_{sc} and PCE of DSSC to some extent; on the contrary, GeW_9 did not show the positive effect, indicating that the transition metal ions may contribute to the catalytic activity.

In summary, two new carboxyethyltin functionalized POMs were synthesized and applied to the CEs of DSSCs when assembled on SWNT electrode for the first time. The composite electrodes show the remarkable catalytic activity toward triiodide reduction and exhibit better photovoltaic performance than Pt electrode owing to the synergy of high electrical conductivity of SWNT and excellent catalytic activity of POM-carboxyethyltin derivatives. This work could provide a new strategy to design promising CE materials with both low cost and high efficiency.

This work was financially supported by the National Natural Science Foundation of China (No. 21131001 and 21201031), Ph. D station Specialized Research Foundation of Ministry of Education for Universities (No. 20120043120007), Science and Technology Development Project Foundation of Jilin Province (No. 201201072), the foundation of China Scholarship Council, and the Analysis and Testing Foundation of Northeast Normal University and the Foundation of Education Department of Liaoning Province (No. L2013414).

Notes and references

[a] *School of Chemistry and Chemical Engineering, Liaoning Normal University, Dalian 116029. E-mail: zhanglancui@lnnu.edu.cn.*
[b] *Key Laboratory of Polyoxometalate Science of Ministry of Education, Department of Chemistry, Northeast Normal University, Changchun, Jilin 130024. E-mail: wangeb889@nenu.edu.cn; chenwl@nenu.edu.cn.*

† Electronic Supplementary Information (ESI) available: Details of the synthesis, structural figures, FTIR, XRPD, TGA, CV and CIF file of the two new POMs; Raman, FTIR, XPS of SWNT/ POM composites; HRTEM of SWNT. See DOI: 10.1039/b000000x/

‡ These authors equally contributed to this communication.

1 (*a*) B. O'Regan and M. Grätzel, *Nature*, 1991, **353**, 737-740; (*b*) A. Yella, H.-W. Lee, H. N. Tsao, C. Yi, A. K. Chandiran, M. K. Nazeeruddin, E. W.-G. Diau, C.-Y. Yeh, S. M. Zakeeruddin and M. Grätzel, *Science*, 2011, **334**, 629-634; (*c*) M. F. He, Z. Q. Ji, Z. J. Huang and Y. Y. Wu, *J. Phys. Chem. C*, 2014, **118** , 16518–16525; (*d*) M.-X. Wu, X. Lin, Y.-D. Wang, L. Wang, W. Guo, D.-D. Qi, X.-J. Peng, A. Hagfeldt, M. Grätzel and T.-L. Ma, *J. Am. Chem. Soc.*, 2012, **134**, 3419-3428; (*e*) Q.-J. Yu, D.-F. Zhou, Y.-S. Shi, X.-Y. Si, Y.-H. Wang and P. Wang, *Energ. Environ. Sci.*, 2010, **3**, 1722-1725; (*f*) X.-J. Zheng, J.-H. Guo, Y.-T. Shi, F.-Q. Xiong, W.-H. Zhang, T.-L. Ma and C. Li, *Chem. Commun.*, 2013, **49**, 9645-9647.

2 (*a*) S. Thomas, T. G. Deepak, G. S. Anjusree, T. A. Arun, S. V. Nair and A. S. Nair, *J. Mater. Chem. A*, 2014, **2**, 4474-4490; (*b*) H.-Q. Fang, C. Yu, T.-L. Ma and J.-S. Qiu, *Chem. Commun.*, 2014, **50**, 3328-3330; (*c*) W.-J. Wang, X. Pan, W.-Q. Liu, B. Zhang, H.-W. Chen, X.-Q. Fang, J.-X. Yao and S.-Y. Dai, *Chem. Commun.*, 2014, **50**, 2618-2620; (*d*) M.-X. Wu, Y.-N. Lin, H.-Y. Guo, K.-Z. Wu and X. Lin, *Chem. Commun.*, 2014, **50**, 7625-7627; (*e*) J. Pan, L.-Z. Wang, J. C. Yu, G. Liu and H.-M. Cheng, *Chem. Commun.*, 2014, **50**, 7020-7023.

3 (*a*) H. N. Tian, Z. Yu, A. Hagfeldt, L. Kloo and L. C. Sun, *J. Am. Chem. Soc.*, 2011, **133**, 9413-9422; (*b*) B. W. Park, M. Pazoki, K. Aitola, S. Jeong, E. M. J. Johansson, A. Hagfeldt and G. Boschloo, *ACS Appl. Mater. Interfaces*, 2014, **6**, 2074-2079; (*c*) H. N. Tsao, J. Burschka, C. Yi, F. Kessler, M. K. Nazeeruddin and M. Grätzel, *Energy Environ. Sci.*, 2011, **4**, 4921-4924.

4 (*a*) L. J. Brennan, M. T. Byrne, M. Bari and Y. K. Gun'ko, *Adv. Energy Mater.*, 2011, **1**, 472-485; (*b*) L.-M. Dai, D. W. Chang, J.-B. Baek and W. Lu, *Small*, 2012, **8**, 1130-1166; (*c*) S. Ahmad, E. Guillen, L. Kavan, M. Grätzel and M. K. Nazeeruddin, *Energ. Environ. Sci.*, 2013, **6**, 3439-3466; (*d*) Z. H. Kang, E. B. Wang, L. Gao, S. Y. Lian, M. Jiang, C. W. Hu and L. Xu, *J. Am. Chem. Soc.*, 2003, **125**, 13652-13653; (*e*) J.-F. Liang, Z. Cai, Y. Tian, L.-D. Li, J.-X. Geng and L. Guo, *ACS Appl. Mater. Interfaces*, 2013, **22**, 12148–12155.

5 G.-R. Li, F. Wang, Q.-W. Jiang, X.-P. Gao and P.-W. Shen, *Angew. Chem. Int. Ed.*, 2010, **49**, 3653-3656.

6 (*a*) H. Lv, J. Song, Y. V. Geletii, J. W. Vickers, J. M. Sumliner, D. G. Musaev, P. Kögerler, P. F. Zhuk, J. Bacsa, G. Zhu and C. L. Hill, *J. Am. Chem. Soc.*, 2014, **136**, 9268-9271; (*b*) X.-B. Han, Z.-M. Zhang, T. Zhang, Y.-G. Li, W. Lin, W. You, Z.-M. Su and E.-B. Wang, *J. Am. Chem. Soc.*, 2014, **136**, 5359-5366; (*c*) Y. Zhu, P.-C. Yin, F.-P. Xiao, D. Li, E. Bitterlich, Z.-C. Xiao, J. Zhang, J. Hao, T.-B. Liu, Y.-G. Wang and Y. Wei, *J. Am. Chem. Soc.*, 2013, **135**, 17155-17160; (*d*) D. L. Long, J. Yan, A. R. Oliva, C. Busche, H. N. Miras, R. J. Errington and L. Cronin, *Chem. Commun.*, 2013,**49**, 9731-9733; (*e*) J. Gao, J. Yan, S. Beeg, D.-L. Long and L. Cronin, *J. Am. Chem. Soc.*, 2012, **135**, 1796-1805; (*f*) M. Carraro, B. S. Bassil, A. Soraru, S. Berardi, A. Suchopar, U. Kortz and M. Bonchio, *Chem. Commun.*, 2013, **49**, 7914-7916; (*g*) P. J. Robbins, A. J. Surman, J. Thiel, D.-L. Long and L. Cronin, *Chem. Commun.*, 2013, **49**, 1909-1911.

7 (*a*) S. Cardona-Serra, J. M. Clemente-Juan, E. Coronado, A. Gaita-Ariño, A. Camón, M. Evangelisti, F. Luis, M. J. Martínez-Pérez and J. Sesé, *J. Am. Chem. Soc.*, 2012, **134**, 14982-14990; (*b*) J. M. Maestre, X. Lopez, C. Bo, J-M. Poblet and N. Casañ-Pastor, *J. Am. Chem. Soc.* ,2001, **123**, 3749-3758.

8 (*a*) C. G. Liu, W. Guan, P. Song, Z. M. Su, C. Yao, E. B. Wang, *Inorg. Chem.*, 2009, **48**, 8115-8119; (*b*) W. Guan, G. C. Yang, L. K. Yan and Z. M. Su, *Inorg. Chem.*, 2006, **45**, 7864−7868.

9 (*a*) A. Dolbecq, P. Mialane, B. Keita and L. Nadjo, *J. Mater. Chem.*, 2012, **22**, 24509; (b) H. L. Li, S. P. Pang, S. Wu, X. L. Feng, K. Müllen and C. Bubeck, *J. Am. Chem. Soc.*, 2011, **133**, 9423-9429.

10 (*a*) J. Friedl, R. Al-Oweini, M. Herpich, B. Keita, U. Kortz, U. Stimming, *Electrochim. Acta*, 2014, **141**, 357-366; (*b*) V. A. Grigoriev, C. L. Hill, I. A. Weinstock, *J. Am. Chem. Soc.*, 2000, **122**, 3544-3545.

11 (*a*) U. Kortz, F. Hussain and M. Reicke, *Angew. Chem. Int. Ed.*, 2005, **44**, 3773-3777; (*b*) C. Boglio, K. Micoine, É. Derat, R. Thouvenot, B. Hasenknopf, S. Thorimbert, E. Lacôte and M. Malacria, *J. Am. Chem. Soc.*, 2008, **130**, 4553-4561; (*c*) S. Bareyt, S. Piligkos, B. Hasenknopf, P. Gouzerh, E. Lacôte, S. Thorimbert and M. Malacria, *J. Am. Chem. Soc.*, 2005, **127**, 6788-6794; (*d*) L.-C. Zhang, S.-L. Zheng, H. Xue, Z.-M. Zhu, W.-S. You, Y.-G. Li and E. Wang, *Dalton. Trans.*, 2010, **39**, 3369-3371; (*e*) X.-J. Sang, J.-S. Li, L.-C. Zhang, Z.-J. Wang, W.-L. Chen, Z.-M. Zhu, Z.-M. Su and E.-B. Wang, *Acs Appl. Mater. Interfaces*, 2014, **6**, 7876-7884.

12 S. Ito, P. Chen, P. Comte, M. K. Nazeeruddin, P. Liska, P. Péchy and M. Grätzel, *Prog. Photovoltaics Res. Appl.*, 2007, **15**, 603-612.

13 C. A. Cooper, R. J. Young, M. Halsall, *Compos., Part A: Appl. Sci. Manuf.*, 2001, **32**, 401-411.

14 J. Kim and A. A. Gewirth, *Langmuir*, 2003, **19**, 8934-8942.

15 L. Xu, H. Zhang, E. Wang, D. G. Kurth and Z. Li, *J. Mater. Chem.*, 2002, **12**, 654-657.

16 J. S. Sanghera, J. Heo and J. D. Mackenzie, *J. Non-cryst. Solids.*, 1988, **101**, 8-17.

17 P.-J. Li, J.-H. Wu, J.-M. Lin, M.-L. Huang, Y.-F. Huang and Q.-H. Li, *Sol. Energy*, 2009, **83**, 845-849.

18 J.-H. Guo, Y.-T. Shi, Y.-T. Chu and T.-L. Ma, *Chem. Commun.*, 2013, **49**, 10157-10159.

19 X.-J. Zheng, J. Deng, N. Wang, D.-H. Deng, W.-H. Zhang, X.-H. Bao and C. Li, *Angew. Chem. Int. Ed.*, 2014, **53**, 7023-7027.